

IDENTIFICATION OF THE SURFICIAL COMPONENT FROM MARTIAN REMOTE SENSING INFRARED SPECTRA: APPLICATION TO Mars Express PFS MEASUREMENTS. A. Maturilli, J. Helbert, and M. D'Amore, Institute for Planetary Research, DLR, Rutherfordstrasse 2, 12489, Berlin, Germany (alessandro.maturilli@dlr.de)

Introduction: Target transformation and factor analysis techniques are applied to the data returned by the Planetary Fourier spectrometer (PFS) on board the ESA Mars Express (MEX) mission. The data analyzed were obtained by the long wavelength channel (LWC) of PFS, in the range roughly from 300 to 1300 cm^{-1} , a region of the spectrum widely used for the presence of diagnostic mineral bands, water and gases spectral features. The principal aims of this work are testing the data analysis technique and applying it to this new dataset. As a starting point we choose the Nili Fossae region, where previous studies (by the OMEGA instrument on MEX) detected phyllosilicates. The result show that the PFS spectrum can be described as linear combination of a limited number of endmembers spectra, representing the varying components present in the observed Martian atmosphere, and one endmember containing the information on surface composition.

For the interpretation of remote sensing measured data an emissivity spectral library of planetary analogue materials is needed. The Berlin Emissivity Database (BED) is focused on relatively fine-grained size separates, providing a realistic basis for interpretation of thermal emission spectra of planetary regoliths, and is therefore complementary to existing thermal emission libraries.

Instrument and Method: The PFS instrument operates since January 2004 on board the MEX spacecraft. The data from the LWC cover the spectral region (dominated by Mars thermal emission) between 270 and 1800 cm^{-1} with a sampling step $\sim 1 \text{ cm}^{-1}$ and an Hamming-apodized spectral resolution of $\sim 2 \text{ cm}^{-1}$. We select only warm diurnal observations [1] where the contribution of the atmospheric constituents could be approximated by a linear fashion model, using appropriate endmember and the scattering by the atmospheric particulates could be neglected.

In the present work a combination of R-mode factor analysis and target transformation are applied to retrieve and characterize the number and the spectral shape of the varying component present in the PFS dataset. These techniques are well established in remote sensing and in laboratory mineral mixtures analysis [2, 3]. The factor analysis tries to find a new basis in which the data can be expressed and where the covariance of the data is minimized.

The eigenvectors and the eigenvalues of the covariance matrix are evaluated and then the covariance matrix is

decomposed in the space generated by the eigenvectors. The eigenvectors corresponding to higher eigenvalues are associated with the most significant information contained in the data. Smaller eigenvalues are associated mainly with noise: finding the crossing point between principal and secondary eigenvalues is the primary task of PCA and involve the user knowledge.

When the eigenvectors, eigenvalues and the minimum number of them needed to describe the data are evaluated, the TT techniques allow the translation to a set of physically meaningful vectors that can be recognized as a spectrum of known material like a mineral or water ice. The transformation is a projection of a set of guess vectors from a reference spectral library, into the vector space generated by the reduced matrix. This process is iterated until a number of independent vectors equal to the estimated data dimensionality is reached.

Laboratory set-up: The instrumentation is located in the Planetary Emissivity Laboratory (PEL) at the Institute for Planetary Research (PF) of the German Aerospace Center (DLR) in Berlin, Germany. It consists of a spectrometer attached to an external emissivity device. The Bruker VERTEX 80v spectrometer, has a very high spectral resolution (better than 0.2 cm^{-1}), and a resolving power of better than 300,000:1, and can be operated under vacuum conditions. To cover the 1 to 16 μm spectral range, a liquid nitrogen cooled MTC detector, a KBr beam-splitter, and a KBr entrance port are used. The 16 to 50 μm spectral range is measured using a room temperature DTGS, a Multi-layer beam-splitter, and a CsI entrance port.

The emissivity device is composed of the sample chamber, a double-walled box with three apertures: a 15 cm squared door used to insert the cup in the box, a 5 cm rounded opening through which the beam is directed to the spectrometer and a 5 cm opening facing the attached blackbody unit. A heater is placed in the chamber and is used to heat the cup with samples from the bottom. The thermal radiation emitted normal to the surface by the sample or the blackbody is collected by an Au-coated parabolic off-axis mirror and reflected to the entrance port of the spectrometer.

A pump circulates water at a constant temperature in the volume between the inner and outer walls of the chamber. The surfaces of the box are painted with black high emissivity paint. The chamber is purged with dry air to remove particulates, water vapour and CO_2 . Further details can be found in [4, 5].

Emissivity of phyllosilicates: The emissivities of our 4 standard grain sizes of the Fe/Mg rich saponite endmember, are shown in Figure 1. A series of diagnostic maxima and minima in emissivity occur in the 3 to 30 μm spectral region, while the rest of the spectra is almost flat and featureless. The Christiansen feature (a maximum in emissivity) is located around 8 μm , corresponding to 1240 cm^{-1} , in total agreement with previous studies [6]. The large adsorption band around 10 μm (1000 cm^{-1}) is due to Si-O stretching, while the Mg_3OH bending vibration is observed at 15.15 μm (660 cm^{-1}). To note is the series of bands between 10 and 14 μm , in particular the change in shape, depending on the grain size, of the band at 11 μm and the shift in the band center position for the 12 μm feature.

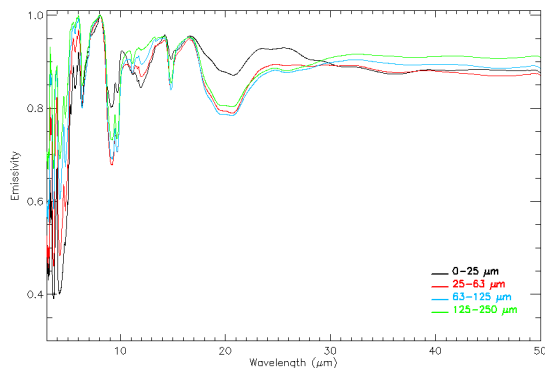


Fig. 1 Emissivity spectra of saponite in the 4 BED grain sizes.

PFS data analysis: Hydrous minerals as phyllosilicates class have been detected on Mars by the OMEGA instrument, onboard the ESA Mars Express mission in the Nili Fossae region, north of Syrtis Major [7, 8]. The OMEGA analysis found a limited range of mineralogy (Fe/Mg and Al smectite), located only in ancient terrains [8]. The recent measurements of the CRISM instrument, onboard the NASA MRO mission, show that the phyllosilicate mineralogy on Mars is wider, giving evidence of kaolinite, chlorite, illite or muscovite, and hydrated silica. Furthermore, nontronite, saponite, and in less amount, chlorite are the most common smectites [9]. We used the previously described method on a set of PFS measurements in the same region where Omega detected the phyllosilicates. Figure 2 shows a picture from [10], showing the Omega map of the region, with PFS footprint superimposed, whose colour represent the intensity of detected phyllosilicates. We maintained the same color code to ease the picture reading.

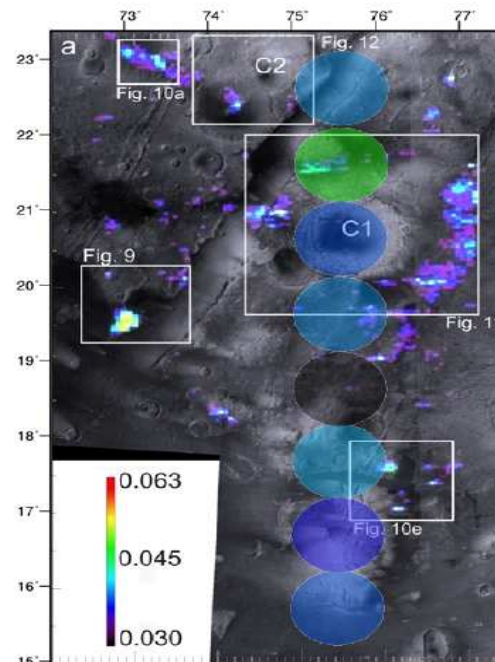


Fig. 2 PFS phyllosilicates identification of a previous Omega detection map.

Conclusion and Outlook: The BED spectral library has been built to analyse the PFS measured spectra, especially for the LWC channel. The first step of this process was to search for confirmation of the OMEGA and CRISM results using factor analysis and target transformation algorithms on PFS data. Future plans include to use the entire database of PFS martian measurements for new investigations.

References: [1] Smith, M. D. et al. (2000) *JGR*, 105, 9589-9607. [2] Bandfield, J. L. et al. (2000) *JGR*, 105, 9573-9587. [3] Ramsey, M. S. and Christensen, P. R. (1998) *JGR*, 103, 577-596. [4] Maturilli A. et al. (2006) *PSS*, 54, 1057-1064. [5] Maturilli A. et al. (2008) *PSS*, 56, 420-425. [6] Koeppen, W. C. and Hamilton V. E. (2005) *JGR*, doi:10.1029/2005JE002474. [7] Bibring J. P. et al. (2005) *Science*, 307, 1576-1581. [8] Poulet F. et al. (2005) *Nature*, 438, 623-627. [9] Mustard J. F. et al. (2008) *Nature*, doi:10.1038/nature07097. [10] Mangold N., et al. (2007) *JGR*, 112.